Received: 9 February 2019 | Revised: 14 January 2020 | Accepted: 20 January 2020

DOI: 10.1002/rnc.4905

RESEARCH ARTICLE

WILEY

Differential flatness-based ADRC scheme for underactuated fractional-order systems

Zongyang Li[1] | Yiheng Wei[1] | Xi Zhou[2] | Jiachang Wang[1] | Jianli Wang[3] | Yong Wang[1]

[1]Department of Automation, University of Science and Technology of China, Hefei, China

[2]Institute of Optics and Electronics, Chinese Academy of Sciences, Chengdu, China

[3]Changchun Institute of Optics, Fine Mechanics and Physics, Chinese Academy of Sciences, Changchun, China

Correspondence

Yong Wang, Department of Automation, University of Science and Technology of China, Hefei, 230026, China.

Email: yongwang@ustc.edu.cn

Funding information

National Natural Science Foundation of China, 61573332, 61601431; Natural Science Foundation of Anhui Province, 1708085QF141

Summary

This article mainly studies the fractional-order active disturbance rejection control (FOADRC) schemes for the underactuated commensurate fractional-order systems (FOSs). The FOADRC framework for linear FOSs-based fractional proportion integration differentiation is constructed by using the fractional-order tracking differentiator and the fractional-order extended state observer, and the necessary conditions for the system to have stable controllers are provided. The FOADRC scheme for underactuated FOSs based on differential flatness is proposed. For underactuated FOSs, a set of flat output expressions with a fixed format is given under the controllable condition of the system. Moreover, making the flat output as the equivalent of the system output is simple and easy to analyze and calculate. Subsequently, the FOADRC scheme is designed by using the flat output. Finally, the scheme proposed in this article is verified by a simulation example.

KEYWORDS

ADRC, differential flatness, fractional calculus, underactuated systems

1 | INTRODUCTION

In the modeling and operation of the actual systems, internal or external disturbance caused by the uncertainty of modeling parameters, aging of components, and other factors exist, thereby causing system performance to degrade. Thus, uncertainties should be considered in the controller design to ensure a desired performance under both disturbances. Hence, it is a meaningful task to study the robust control problem for those disturbed systems.

To improve the robustness of the system, we mainly proceed from two aspects, namely, modeling and control schemes. In terms of modeling, as a generalization from traditional calculus, fractional calculus enjoys both conciseness and veracity in complex system modeling, parameter estimation and control.[1-3] Fractional-order system (FOS) theory, as well as fractional-order controller design, has attracted lots attention in recent years. It is shown that fractional-order control (FOC) owns a higher degree of freedom than integer ones in controller parameters selection, and therefore owns a greater potential in system performance improvement. As we become more demanding on model accuracy and control performance, FOS theory[4-7] and fractional-order controller design have developed rapidly in recent years. In terms of control schemes for FOSs, many schemes[8-11] are proposed to deal with the internal or external disturbance, among them, fractional-order proportion integration differentiation (PID) and CRONE[12] have been widely used, but both schemes have limitation. Han proposed active disturbance rejection control (ADRC)[13] in 1998, comparing to other control schemes, ADRC has outstanding advantages in dealing with robust control of uncertain systems with large-scale and complex structures.[14,15] Actually, because of its simple structure, simple feedback and good dynamic performance, fractional-order active disturbance rejection control (FOADRC) has been widely used too. On the one hand, it can effectively solve the contradiction between the rapidity and overshoot by arranging the transition process. On the other hand, the idea of disturbance compensation can be extremely to improve the robustness of the controlled system. FOADRC is a combination of fractional-order modeling and ADRC, and there have been some research results in the study of FOADRC. Li et al[16] designed an integer ADRC controller for fractional-order controlled objects. Erenturk proposed a FOADRC scheme for integer-order systems and changed the PID feedback control to the $\mathrm{PI}^{\lambda}\mathrm{D}^{\mu}$ control, and he designed an ADRC scheme for a nonlinear drive system.[17] There are also references[18,19] using fractional-order PID control scheme to control integer-order systems. The above research only deals with the fractional-order dynamics as a disturbance or only involves FOC in the feedback control, the fractional modules are not considered to construct the framework of ADRC. In fact, Yiheng Wei proposed an fractional-order tracking differentiator (FOTD),[20,21] then Zhe proposed an fractional-order extended state observer (FOESO) and a $PI^{\lambda}D^{\mu}$ feedback controller, build the preliminary framework of FOADRC,[22] and it is used to the synchronous control of chaotic systems.[23] At present, the research and applications of ADRC schemes still focus on integer-order systems, a rare FOADRC schemes are still limited to integer-order systems. Although the ADRC framework of the FOSs has preliminary conclusions, it is aimed at SISO or simpler decoupled MIMO systems. For complex FOSs, there are some vacancies in ADRC schemes.

Underactuated mechanical systems are often used to reduce manufacturing cost and the impact of weight on system stability in actual engineering. Thus, we select an underactuated system as our research object. In an underactuated system, the dimension of the generalized coordinate vector space of the system is higher than the dimension of the control input signal. For example, the inverted pendulum system is a typical underactuated system. The input control signal needs to simultaneously control the angle of the pendulum and the displacement of the car;[24] in a common ship system, the propulsion device is only propeller and rudder, but the propeller and the rudder need to simultaneously control the displacement and angle in two directions of the ship, which is also an underactuated system. For such underactuated systems, differential flatness features can be used for processing. In studying of fractional differential flatness, some calculation methods and applications of fractional flat output are available.[25-28] The basic idea is to dynamically extend a class of nonlinear systems with incomplete feedback linearization in the sense of differential homeomorphism and avoid the complicated integration process,[29] but not all systems are differentially flat systems, and its flat output is not unique and difficult to find even if it is a differentially flat system. Victor et al[27] give a characterization of fractionally flat outputs and a simple algorithm to compute them. They also obtained a characterization of the so-called fractionally 0-flat outputs in the framework of polynomial matrices of the fractional derivative operator. This work also introduces a method for computing the fractional flat outputs based on the existing literature.[25]

For the above problems, the main contributions of this article can be summarized in three aspects. First, the FOADRC framework for the linear FOSs is based on PID control and constructed by using FOTD and FOESO, the necessary conditions for the existence of stable parameters for the controller are provided. Second, a set of flat output expressions with a fixed format can be given under the controllable conditions for underactuated FOSs, thereby making the analysis and calculation of flat output as the equivalent of the system output simple and easy, and the FOADRC scheme for underactuated FOSs is designed by using the flat output. Third, the scheme proposed in this article is verified by a simulation example. The remainder of this article is organized as follows. In Section 2, preliminaries, such as fractional-order PID, FOTD and FOESO, are introduced. The main results of this article are given in Section 3. A simulation example is given in Section 4 to verify the proposed control scheme. Finally, Section 5 is the conclusion.

2 | PRELIMINARIES

ADRC mainly contains three parts: TD, it is used to arrange a transition process for the reference signal and give a differential signal. Another is ESO, it is used to estimate the state variables and total disturbances. As for the controller, the most commonly used controller for ADRC is a nonlinear or linear PID controller, which take the error of the system as input to make the system track the error signal. Given that, the block diagram of the integer-order ADRC is similar to the block diagram of the fractional-order ADRC, and the basic idea is also consistent. Thus, each module in the integer-order ADRC is not separately introduced. In the fractional domain, when the controlled system is fractional, the TD, the ESO and the control law are also fractional; hence, introducing FOTD and FOESO is necessary.

In this article, if no special instructions, then the listed FOS states refer to the pseudo state of the system represented by the state space equation rather than the true states.

2.1 | Fractional-order PID controller

The fractional differential used in this article is defined as follows.

Definition 1. Real function $f(t)$ is absolutely integrable and has mth-order continuous derivative in $t > 0$. Its Caputo fractional differential is defined as

$$ {}_{c}^{C}\mathscr{D}_{t}^{\alpha} f(t) = {}_{c}^{R}\mathscr{I}_{t}^{m-\alpha}\left[\mathscr{D}^{m} f(t)\right] = \frac{1}{\Gamma(m-\alpha)} \int_{c}^{t} \frac{f^{(m)}(\tau)}{(t-\tau)^{\alpha-m+1}} d\tau, \tag{1} $$

where m is a positive integer and satisfies $m - 1 < \alpha \leq m$.

Therefore, in the absence of special instructions, this article uses Definition 1. If $c = 0$ is used as the initial instant, then the integral operator is abbreviated as $\mathscr{I}^{\alpha}$, and the differential operator is abbreviated as $\mathscr{D}^{\alpha}$.

In the field of integer-order control, PID controllers are widely used in engineering projects, and scholars have also conducted extensive research on selecting suitable PID controller parameters. Subsequently, Podlubny tried to extend the order of the controller and proposed a fractional-order PID controller, that is, the famous $PI^{\lambda}D^{\mu}$ controller.[30] Compared with the traditional PID controllers, the $PI^{\lambda}D^{\mu}$ controller introduces λ and μ and increases the adjustable parameters of the controller. Subsequently, the parameter tuning range is expanded, the flexibility of the controller is expanded, and improved robustness is exhibited. For integer-order PID controllers, the order of their integral and differential can only be selected as 0 or 1. However, the integral and differential orders of fractional $PI^{\lambda}D^{\mu}$ controllers can be arbitrarily selected within an interval. The transfer function of $PI^{\lambda}D^{\mu}$ controller is

$$ C(s) = k_p + \frac{k_i}{s^{\lambda}} + k_d s^{\mu}, \quad \lambda > 0, \quad \mu > 0, \tag{2} $$

where λ and μ can be any nonnegative real numbers, and k_p, k_i, and k_d are the controller proportional factor, integral coefficient, and differential coefficient, respectively. In the time domain analysis, assuming that the system tracking error is $e(t)$, then the control signal $u(t)$ of the $PI^{\lambda}D^{\mu}$ controller can be written as

$$ u(t) = k_p e(t) + k_i \mathscr{I}^{\lambda} e(t) + k_d \mathscr{D}^{\mu} e(t). \tag{3} $$

The traditional PID control is a special case of $PI^{\lambda}D^{\mu}$ control actually. In the controlled systems, different λ and μ also can be designed to achieve improved control effects except for three gains.

2.2 | Fractional-order tracking differentiator

Considering the tracking problem of a 2αth-order linear system, and the order of the reference signal $v(t)$ is $0 < \alpha < 1$. Let state $v_1(t)$ track the reference signal $v(t)$, where the control input $|u(t)| \leq r$,

$$ \begin{cases} \mathscr{D}^{\alpha} v_1(t) = v_2(t), \\ \mathscr{D}^{\alpha} v_2(t) = u(t). \end{cases} \tag{4} $$

The optimal control law can be obtained by using the principle of minimization[31]

$$ u^{*}(t) = -r\,\mathrm{sgn}\left(v_1(t) - v(t) + A v_2(t) |v_2(t)|\right), \tag{5} $$

$$ A = \frac{1}{r} - \frac{\Gamma^2(\alpha+1)}{r\Gamma(2\alpha+1)}. \tag{6} $$

Substitute this optimal control law into system (4), under the condition of $\left|\mathscr{D}^{2\alpha} v_1(t)\right| \leq r$, the state $v_1(t)$ can track the reference input signal $v(t)$, and state $v_2(t)$ is the αth-order differential of state $v_1(t)$, which can be approximated as the

αth-order differential of the reference input $v(t)$

$$v_1(t) \approx v(t), \quad v_2(t) \approx \mathscr{D}^\alpha v(t), \tag{7}$$

thus, system (4) is an FOTD under the control law (5).

However, the symbolic function $\mathrm{sgn}(\cdot)$ can easily to make the system state response chatter, then its use in practical projects is impractical; hence, a saturation function can be introduced to replace the symbolic function. The FOTD that uses the saturation function is as expressed as follows

$$\begin{cases} \mathscr{D}^\alpha v_1(t) = v_2(t), \\ \mathscr{D}^\alpha v_2(t) = -r sat\left(v_1(t) - v(t) + A v_2(t)\left|v_2(t)\right|\right), \end{cases} \tag{8}$$

and the saturation function is presented as follows

$$sat(x) = \begin{cases} x/\varepsilon, & |x| < \varepsilon, \\ \mathrm{sgn}(x), & |x| \geq \varepsilon, \end{cases} \tag{9}$$

where ε is a constant greater than 0 but very close to 0.

Because the saturation function will make calculations complicated in the simulation, another idea to solve the chattering problem caused by the symbolic function is to use a hyperbolic tangent function instead of a symbolic function, then the selected FOTD is as follows

$$\begin{cases} \mathscr{D}^\alpha v_1(t) = v_2(t), \\ \mathscr{D}^\alpha v_2(t) = -r \tanh\left[k\left(v_1(t) - v(t) + A v_2(t)\left|v_2(t)\right|\right)\right], \end{cases} \tag{10}$$

and the hyperbolic tangent function can be expressed as

$$\tanh(x) = \frac{e^x - e^{-x}}{e^x + e^{-x}}, \quad x \in \mathbb{R}, \tag{11}$$

the larger k, the closer the performance of the hyperbolic tangent function is to the performance of the sign function $\mathrm{sgn}(\cdot)$ and the faster the reference signal is tracked. The larger the k in the FOTD (10), the faster the system will be tracked. At the same time, the parameter r is the boundary value of the bounded control input $u(t)$ in FOTD, and it determines the speed of state $v_1(t)$ tracking reference signal $v(t)$, the larger r, the faster the tracking speed. However, it should be noted that if r is too large, then it will cause amplification of the disturbance signal in the reference signal $v(t)$. Therefore, when selecting the value of r, both tracking speed and signal disturbance need to be considered.

In fact, the FOTD cannot only obtain the differential signal of the reference signal, but also has an effect on the overarrangement of the reference signal. The response speed can still be guaranteed under the influence of the transition process, while the overshoot problem can be solved. Given that the tracked differential signal is no longer a first-order differential signal, but an αth-order differential signal with $0 < \alpha < 1$, and its value cannot be 0 when tracking an αth-order differential signal of a constant signal.

2.3 | Fractional-order extended state observer

A commensurate nonlinear FOS with the state $x(t) = [x_1(t), x_2(t), \ldots, x_n(t)]$

$$\begin{cases} \mathscr{D}^\alpha x_i(t) = x_{i+1}(t), i = 1, 2, 3, \ldots, n-1, \\ \mathscr{D}^\alpha x_n(t) = f\left(x_1(t), x_2(t), \ldots, x_n(t)\right) + b u(t) + w(t), \\ y(t) = x_1(t), \end{cases} \tag{12}$$

where $0 < \alpha < 1$ and $b \neq 0$, $f(x_1(t), x_2(t), \ldots, x_n(t))$ is a known (or unknown) nonlinear (or linear) function for the system state $x(t)$, and $w(t)$ is the total external disturbance of the system. Define an extended state $x_{n+1}(t) = f(x_1(t), x_2(t), \ldots, x_n(t)) + w(t)$, then the FOESO is as follows[22]

$$\begin{cases} \mathscr{D}^{\alpha} z_i(t) = z_{i+1}(t) - \beta_i \varepsilon_1(t), i = 1, 2, 3, \ldots, n-1, \\ \mathscr{D}^{\alpha} z_n(t) = z_{n+1}(t) - \beta_n \varepsilon_1(t) + bu(t), \\ \mathscr{D}^{\alpha} z_{n+1}(t) = -\beta_{n+1} \varepsilon_1(t). \end{cases} \tag{13}$$

$\varepsilon_i(t)$ is the error signal, and $\varepsilon_i(t) = z_i(t) - x_i(t)$, among them $i = 1, 2, \ldots, n+1$. If $h(t) = \mathscr{D}^{\alpha} x_{n+1}(t)$ is defined as an input signal, then use system (13) minus system (12) to get the error signal system. The characteristic function of its state matrix is $F(s) = s^{(n+1)\alpha} + \beta_1 s^{n\alpha} + \beta_2 s^{(n-1)\alpha} + \ldots + \beta_{n+1}$. We generally take $F(s) = (s^{\alpha} + \omega_o)^{n+1}$ for convenience of analysis, that is,

$$\beta_i = C_{n+1}^{i} \omega_0^{i}, \quad i = 1, 2, \ldots, n+1. \tag{14}$$

It can be proven that FOESO (13) is stable in BIBO, and the error between the observed state and the original system is bounded when $|h(+\infty)| \leq M$ and satisfies

$$|\varepsilon_i(\infty)| \leq \frac{M C_{n+1}^{i-1}}{\omega_0^{n+2-i}}. \tag{15}$$

In the FOESO, the value of ω_0 is positively correlated with the convergence rate of the observer. As ω_0 increases, the convergence speed of the observer will also rise. However, an oversized ω_0 value will also amplify the noise of the sensor. Therefore, we should select the appropriate value of ω_0.

3 | MAIN RESULTS

3.1 | Linear FOADRC

In the fractional-order PID control theory, the FOADRC framework is shown in Figure 1. $z_i(t)$ and $z_{n+1}(t)$ can be obtained by FOESO (13). $z_i(t) \approx x_i(t), i = 1, 2, \ldots, n$ is the approximation of the system state and $z_{n+1}(t) \approx f(x_1(t), x_2(t), \ldots, x_n(t)) + w(t)$ is the approximation of the sum of the nonlinear function $f(\cdot)$ and the external perturbation$w(t)$. According to Figure 1, a PI$^{\lambda}$D$^{\mu}$ controller can be designed as

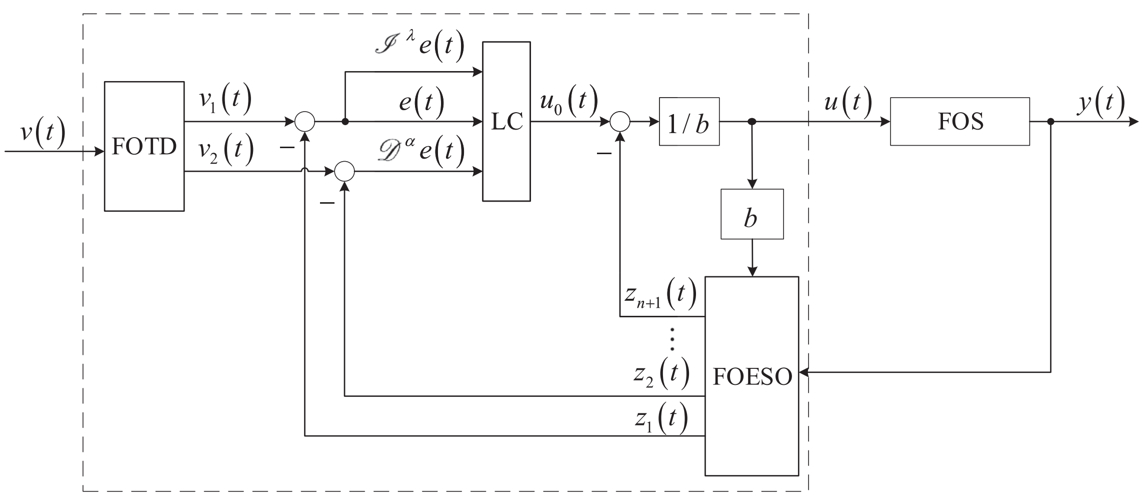

FIGURE 1 System block diagram of fractional-order active disturbance rejection control

$$bu_0(t) = k_p e_1(t) + k_i \mathscr{I}^{\lambda} e_1(t) + k_d e_2(t), \tag{16}$$

$$u(t) = u_0(t) - \frac{z_{n+1}(t)}{b}, \tag{17}$$

where the order of the controller is selected as $\mu = \alpha$, and the error signal is defined as $e_1(t) = v_1(t) - z_1(t)$, $e_2(t) = v_2(t) - z_2(t)$. $v_1(t)$ is the tracking signal of the system reference input signal $v(t)$. $v_2(t)$ is an αth-order differential of $v_1(t)$ and it can be generated by the FOTD. Substitute the above controller into the system output equation $y(t) = x_1(t)$ and make an $n\alpha$-order differential, then its output $y(t)$ can be approximated as

$$\mathscr{D}^{n\alpha} y(t) = f(x_1(t), x_2(t), \ldots, x_n(t)) + w(t) + bu(t) \approx bu_0(t). \tag{18}$$

Finding that item $z_{n+1}(t)/b$ can fully compensate for the impact of the nonlinear item and the external disturbance of the system in (17), and this reason causes why the nonlinear function $f(\cdot)$ is not a known function, but does not affect the result of the controller design.

There are approximate relationships $e_1(t) \approx v(t) - y(t)$ and $e_2(t) \approx \mathscr{D}^{\alpha}(v(t) - y(t))$ in the above system. If the controlled system is an SISO system and the Laplace transform of the above approximation system is taken, then the transfer function of the closed-loop system can be obtained as follows

$$H(s) = \frac{Y(s)}{V(s)} = \frac{k_d s^{\alpha+\lambda} + k_p s^{\lambda} + k_i}{s^{\alpha n+\lambda} + k_d s^{\alpha+\lambda} + k_p s^{\lambda} + k_i}. \tag{19}$$

Furthermore, if the above transfer function is treated as a closed-loop transfer function obtained after a unit of negative feedback from an open-loop system, then the equivalent open-loop transfer function of the system can be obtained

$$F(s) = \frac{k_d s^{\alpha+\lambda} + k_p s^{\lambda} + k_i}{s^{\alpha n+\lambda}}. \tag{20}$$

Parameter n and parameter α are determined by the controlled system. The system can be controlled stably by configuring the appropriate quaternion parameter group (k_p, k_i, k_d, λ). For the selection of the parameters (k_p, k_i, k_d, λ), the inference is in the following

Corollary 1. *For an n-dimensional commensurate FOS, n is greater than 1, the necessary condition for the system to have a stable $PI^{\lambda}D^{\mu}$ controller for FOADRC is that there is an integer a, the dimension n and the order α of the system satisfies the inequality relation* $4a/(n-1) < \alpha < 2(2a+1)/(n-1)$.

In fact, the stable domain of controller parameters in the parameter plane is related to the real root boundary (RRB), complex root boundary (CRB), and infinite root boundary of the system closed-loop characteristic equation.[32] The characteristic equation of the closed-loop system (19) is $s^{\alpha n+\lambda} + k_d s^{\alpha+\lambda} + k_p s^{\lambda} + k_i = 0$, and the real part $\mathrm{Re}(\omega)$ and the imaginary part $\mathrm{Im}(\omega)$ of the frequency can be obtained by frequency domain decomposition. If the values of (k_p, λ) are taken as determined positive numbers, then we can get the expression of the other two parameters

$$k_i(\omega) = \left[\omega^{\alpha n+\lambda} \sin\frac{\alpha\pi(n-1)}{2} - k_p \omega^{\lambda} \sin\frac{\alpha\pi}{2}\right] \csc\frac{(\alpha+\lambda)\pi}{2}, \tag{21}$$

$$k_d(\omega) = \left[-\omega^{\alpha(n-1)} \sin\frac{(\alpha n+\lambda)\pi}{2} - k_p \omega^{-\alpha} \sin\frac{\lambda\pi}{2}\right] \csc\frac{(\alpha+\lambda)\pi}{2}, \tag{22}$$

the corresponding multiroot boundary curve $(k_i(\omega), k_d(\omega))$ and the RRB curve $k_i(\omega) = 0$. The stable domain of the controller parameters $(k_i(\omega), k_d(\omega))$ is the intersection of the left side of the CRB curve and the right side of the RRB curve. Obviously the right side of the RRB curve corresponds to the controller parameter $k_i > 0$, for the $k_i(\omega)$ expression (21), the inequality $\omega^{n\alpha} \sin\alpha\pi(n-1)/2 > k_p \sin\alpha\pi/2 > 0$ must be satisfied to make $k_i > 0$ solution. Therefore, it must be guaranteed that $\sin\alpha\pi(n-1)/2 > 0$. The restrictions of the system order can be obtained by calculating.

From the above analysis, it can be seen that when the $PI^{\lambda}D^{\alpha}$ controller is selected as the feedback controller in the FOADRC, there are restrictions for the dimension and order of the system. When the system dimension $n \leq 3$, the condition in Corollary 1 is satisfied, and therefore the corresponding stable controller parameters can be found. It should be noted that when the system order is higher, it must be first verified whether a stable controller can be found, if not, we need to select other control schemes, such as nonlinear PID control.

On the other hand, we can see that the relative order of the system under the FOADRC framework is $\alpha(n-1)$ from the system equivalent transfer function (19) and (20). When α is larger, the order of the system is also higher, and its performance is similar to the high-order integral, and the system has obvious overshoots and oscillations. When α is very small, such as $\alpha < 1/(n-1)$, the system behaves like a FOS with the order less than 1. Although the system does not have overshoots and oscillations, its convergence rate is much slower than integer first-order system. Combined with Corollary 1, if the system order and dimension satisfy $1/(n-1) < \alpha < 2/(n-1)$, the stability and response speed are guaranteed. In particular, the closer the order α is to $1/(n-1)$, the better the system performs at overshoots and convergence speed. When $n = 2$, the FOS is a 2α-order system and $2\alpha \in (0, 2)$, obviously for different values of α, the dynamic performance exhibited by the system may be similar to a first-order system or a second-order system, and also confirms the diversity of dynamic performance exhibited by the FOSs.

The stability of the system can also be confirmed from the frequency domain analysis by using an $n\alpha$th-order system as an example and $n = 2$, $\alpha = 0.5$. The Bode diagram of different controller parameters is shown in Figure 2. In each Bode diagram, with the exception of specific parameters, the rest of the parameters are fixed values, $(k_p, k_i, k_d, \lambda) = (1, 1, 1, 0.8)$.

It can be seen from the figure that the change of the parameter λ has little effects on the crossover frequency and phase margin of the open-loop system. The changes of the parameter k_p and parameter k_i will cause the system to cross the

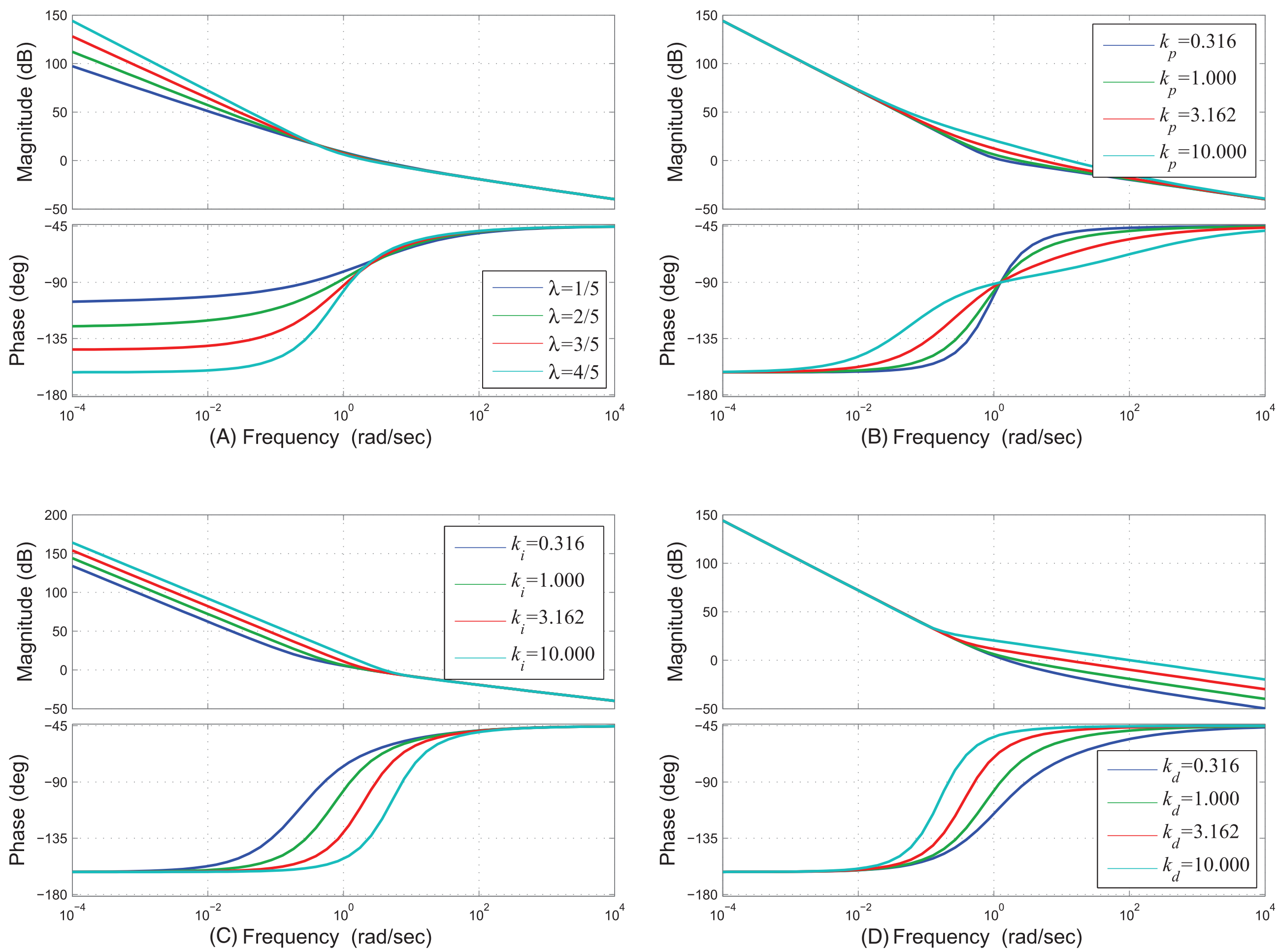

FIGURE 2 Bode diagrams of open-loop system with different parameter configurations (A, λ; B, k_p; C, k_i; D, k_d) [Colour figure can be viewed at wileyonlinelibrary.com]

frequency point. However, the phase margin at the corresponding crossover frequency point remains almost the same; in contrast, only the parameter k_d has a significant influence on the system crossover frequency point and phase margin, which also indirectly indicates the FOADRC has good robustness to the control parameters $\left(k_p, k_i, \lambda\right)$. In the actual engineering, the CRB and the RRB curve can be drawn by selecting a specific $\left(k_p, \lambda\right)$ value to find a suitable controller parameter (k_i, k_d). At the same time, to ensure the good performance of the system, the parameter values far from the CRB and the RRB curve should be selected as far as possible.

3.2 | Flat output of linear FOSs

Consider the fractional-order commensurate linear equation of states

$$\mathscr{D}^{\alpha}x(t) = Ax(t) + Bu(t), \tag{23}$$

where $0 < \alpha \leq 2, A \in \mathbb{R}^{n\times n}, B \in \mathbb{R}^{n\times 1}$ and $x(t) \in \mathbb{R}^n$.

Definition 2. Consider the commensurate FOS[25]

$$\mathscr{D}^{\alpha}x(t) = f(x(t), u(t)), \tag{24}$$

where $x(t) = [x_1(t), x_2(t), \ldots, x_n(t)] \in \mathbb{R}^n$ and $u(t) = [u_1(t), u_2(t), \ldots, u_m(t)] \in \mathbb{R}^m$, $f = (f_1, f_2, \ldots, f_n)$ is a regular function for x, u and $\partial^{\alpha}f/\partial u^{\alpha}$ has a rank of m. If we can find a set of output $z(t) = h\left(x(t), u(t), \mathscr{D}^{\alpha}u(t), \ldots, \mathscr{D}^{\beta\alpha}u(t)\right) \in \mathbb{R}^m$, such that all states $x_i(t)$ and input $u_j(t)$ can be expressed as suitable functions of $z(t)$ and its finite αth-order derivatives, that is,

$$\begin{aligned} x_i(t) &= p_i\left(z(t), \mathscr{D}^{\alpha}z(t), \ldots, \mathscr{D}^{p\alpha}z(t)\right), \\ u_i(t) &= q_i\left(z(t), \mathscr{D}^{\alpha}z(t), \ldots, \mathscr{D}^{q\alpha}z(t)\right), \end{aligned} \tag{25}$$

where β is a positive integer, then system (24) is said to be differentially (fractionally) flat, and $z(t)$ is its fractionally linear flat output. When $\beta = -1$, that is, $z(t) = h(x(t))$, system (24) is said to be differentially (fractionally) 0-flat.

Lemma 1. [25] *System* (23) *is differentially (fractionally) flat if and only if* $n \times m$*-dimensional matrix* $P(s^{\alpha})$ *and* $m \times m$*-dimensional matrix* $Q(s^{\alpha})$ *satisfy*

$$\begin{aligned} R^T\left[s^{\alpha}I_n - A\right]P(s^{\alpha}) &= 0, \\ \left[s^{\alpha}I_n - A\right]P(s^{\alpha}) &= BQ(s^{\alpha}), \end{aligned} \tag{26}$$

where R *is an arbitrary matrix orthogonal to* B*, and* $\text{rank}(R) = n - m$. $P(s^{\alpha})$ *and* $Q(s^{\alpha})$ *are called definition matrices, and their ranks are all* m.

In fact, according to the definition of the differential flatness and the flat output, if z is a flat output of system (23), then there must be function groups $p_i(\cdot)$ and function groups $q_i(\cdot)$ satisfying (25). Take Laplace transform of (25), matrices $P(s^{\alpha})$ and $Q(s^{\alpha})$ must satisfy

$$X(s) = P(s^{\alpha})Z(s), \quad U(s) = Q(s^{\alpha})Z(s). \tag{27}$$

Substitute the above equations into the Laplace transform of system (23), then we can get $[s^{\alpha}I_n - A]P(s^{\alpha}) = BQ(s^{\alpha})$. On the other hand, if there is a matrix R orthogonal to B, then there are $R^TB = 0$ and $R^T[s^{\alpha}I_n - A]P(s^{\alpha}) = R^TBQ(s^{\alpha}) = 0$.

Therefore, if we can find the matrices $P(s^{\alpha})$ and $Q(s^{\alpha})$ obtained from the Laplace transformation of the function groups $p_i(\cdot)$ and $q_i(\cdot)$ satisfying (25) and a matrix R orthogonal to B, then a flat output of system (23) must exist. There is a Laplace relationship between the expected output and the flat output for a differentially (fractionally) flat system

$$Y(s) = CP(s^{\alpha})Z(s) + DQ(s^{\alpha})Z(s) \triangleq W(s^{\alpha})Z(s). \tag{28}$$

Lemma 2. *[25] A linear flat output defines an output defined by* $z(t) = h\left(x(t), u(t), \mathscr{D}^{\alpha}u(t), \dots, \mathscr{D}^{\beta\alpha}u(t)\right) \in \mathbb{R}^m$ *with h being linear. If system* (23) *is controllable, it must have linear flat output and its defining matrices P and Q.*

Lemma 3. *[33] A commensurate FOS with n-dimensional states is fully controllable if and only if its controllability matrix*

$$M_c = \left[B, AB, A^2B, \dots, A^{n-1}B\right] \tag{29}$$

is full rank.

Theorem 1. *If the single-input FOS (23) is a controllable system under the zero initial conditions, then a flat output* $z(t)$ *satisfying* (26) *must exist.* $z(t)$, $P(s^{\alpha})$, $Q(s^{\alpha})$, *and R are as follows*

$$z(t) = [1, 0, \dots, 0]\, T^{-1}M_c^{-1}x(t), \tag{30}$$

$$P(s^{\alpha}) = M_c T\left[1, s^{\alpha}, \dots, s^{(n-1)\alpha}\right]^T, \tag{31}$$

$$Q(s^{\alpha}) = [0, \dots 0, 1]\left[s^{\alpha}I_n - T^{-1}M_c^{-1}AM_cT\right]\left[1, s^{\alpha}, \dots, s^{(n-1)\alpha}\right]^T, \tag{32}$$

$$R^T = [m_1, m_2, \dots, m_{n-1}, 0]\, T^{-1}M_c^{-1}. \tag{33}$$

The expressions for M_c *and T are as follows*

$$M_c = \left[B, AB, \dots, A^{n-1}B\right], \quad T = \begin{bmatrix} a_1 & a_2 & \dots & a_{n-1} & 1 \\ a_2 & a_3 & \dots & 1 & \\ \vdots & \vdots & \iddots & & \\ a_{n-1} & 1 & & & \\ 1 & & & & \end{bmatrix}, \tag{34}$$

$a_i\,(i = 1, 2 \dots n-1)$ *are the coefficients of the characteristic polynomial of the matrix A for* $\lambda = s^{\alpha}$, *that is,*

$$f_A(\lambda) = \lambda^n + a_{n-1}\lambda^{n-1} + \dots + a_1\lambda + a_0, \tag{35}$$

$m_i\,(i = 1, 2 \dots n-1)$ *are real numbers and are not all zeros.*

Proof. The controllability matrix M_c must be full rank according to Lemma 3 because FOS (23) is controllable. If the column vectors in M_c are regrouped in the following manner, then the new n-dimensional column vectors must also be linearly independent.

$$\begin{cases} p_i = a_iB + a_{i+1}AB + \cdots + a_{n-i}A^{n-1-i}B + A^{n-i}B, i = 1, 2, 3, \dots, n-2, \\ p_{n-1} = a_{n-1}B + AB, \\ p_n = B. \end{cases} \tag{36}$$

If use p_i to construct a matrix $E = \left[p_1, p_2, \dots, p_n\right]$, it is obviously that $E = M_cT$ and the matrix is a full rank matrix.

We take $A_c = E^{-1}AE$ and $B_c = E^{-1}B$, where A_c is an nth-order square matrix, and B_c is a column vector, then it can be proved by calculation

$$A_c = \begin{bmatrix} 0 & 1 & 0 & \dots & 0 \\ 0 & 0 & 1 & \dots & 0 \\ \vdots & \vdots & \vdots & \ddots & \vdots \\ 0 & 0 & 0 & \dots & 1 \\ -a_0 & -a_1 & -a_2 & \dots & -a_{n-1} \end{bmatrix}, \quad B_c = \begin{bmatrix} 0 \\ 0 \\ \vdots \\ 0 \\ 1 \end{bmatrix}. \tag{37}$$

We take the n-dimensional variables $v(t) = E^{-1}x(t)$, and take the first item of the variables $v(t)$ as the flat output, that is, $z(t) = [1, 0, \dots, 0]\, v(t)$. $Z(s) = [1, 0, \dots, 0]\, E^{-1}X(s)$ can be obtained by Laplace transform, and both sides of this equation is multiplied by s^{α}. The Laplace transform of the original system (23) is substituted into this equation, then $E^{-1}A = A_cE^{-1}$, and we can obtain $s^{\alpha}Z(s) = [1, 0, \dots, 0]\, A_cE^{-1}X(s) + [1, 0, \dots, 0]\, B_cU(s) = [0, 1, \dots, 0]\, E^{-1}X(s)$. Furthermore, we multiply both sides of this equation by s^{α} and repeat the above process until we obtain $s^{(n-1)\alpha}Z(s)$. Finally, we can get

$$\begin{bmatrix} Z(s) \\ s^{\alpha}Z(s) \\ \vdots \\ s^{(n-1)\alpha}Z(s) \end{bmatrix} = \begin{bmatrix} 1 & 0 & \dots & 0 \\ 0 & 1 & \dots & 0 \\ \vdots & \vdots & \ddots & \vdots \\ 0 & 0 & \dots & 1 \end{bmatrix} E^{-1}X(s) \Rightarrow X(s) = E \begin{bmatrix} 1 \\ s^{\alpha} \\ \vdots \\ s^{(n-1)\alpha} \end{bmatrix} Z(s). \tag{38}$$

We can obtain the specific expression of the matrix $P(s^{\alpha})$, as shown in (31). Multiply $s^{(n-1)\alpha}Z(s)$ by s^{α} and substitute $s^{(n-1)\alpha}Z(s)$ into the Laplace transform of the original system

$$s^{n\alpha}Z(s) = [0, \dots, 0, 1]\, A_cE^{-1}X(s) + U(s). \tag{39}$$

By substituting (38) into the above formula, the following equation can be obtained

$$Q(s^{\alpha}) = [0, \dots, 0, 1] \left[s^{\alpha}I_n - A_c\right] \left[1, s^{\alpha}, \dots, s^{(n-1)\alpha}\right]^T. \tag{40}$$

By substituting A_c into the above formula, the expression (32) of the matrix $Q(s^{\alpha})$ can be obtained.

In addition, $m_i\,(= 1, 2 \dots n-1)$ is not all zeros, and $M = [m_1, \dots, m_{n-1}, 0]$ is obviously a vector, that is, orthogonal to B_c satisfies $MB_c = ME^{-1}B = 0$. If let $R^T = ME^{-1}$, that is,

$$R^T \left[s^{\alpha}I_n - A\right] P(s^{\alpha}) = R^TBQ(s^{\alpha}) = ME^{-1}BQ(s^{\alpha}) = 0. \tag{41}$$

The variable $z(t)$ and its Laplace transform $Z(s)$ satisfy (26) in Lemma 1, so it is a set of flat output of system (23). ■

It can be found that the flat output is the first state variable of the controllable standard system after the linear transformation of the original system from the proof, and the state $v(t)$ satisfies the following differential equation

$$\mathscr{D}^{\alpha}v(t) = A_cv(t) + B_cu(t). \tag{42}$$

According to the existing literature,[34] the controllability matrix (29) for the multiinput controllable FOS $\mathscr{D}^{\alpha}x(t) = Ax(t) + Bu(t)$, $B = (b_1, b_2, \dots, b_m)$ (b_i are column vectors) can be written as

$$M_c = \left[b_1, \dots, b_m, Ab_1, \dots, Ab_m, \dots, A^{n-1}b_1, \dots, A^{n-1}b_m\right]. \tag{43}$$

Since the system is controllable, from the columns of the matrix M_c, we construct a basis for the n-vector space M_R. We examine the column vectors of M_c in the order specified by (43). We accept a vector, which is examined as a vector of the basis if it is linearly independent of all those previously accepted, otherwise we reject it. When n vectors have been accepted we rearrange

$$M_R = \left[b_1, Ab_1, \dots A^{r_1-1}b_1, b_2, Ab_2, \dots A^{r_2-1}b_2, \dots, b_m, Ab_m, \dots A^{r_m-1}b_m\right], \tag{44}$$

where $r_1 + r_2 + \dots + r_m = n$. Then, the corresponding coefficients $r_1, r_2, \dots, r_m$ are the controllability indices of the system. Furthermore, the controllability indices set is defined as $r = \max\{r_1, r_2, \dots, r_m\}$.

Theorem 2. *If a multiinput commensurate FOS (23) is controllable under the zero initial conditions, there is a group of flat output $z(t)$ satisfies Lemma 1. $z(t)$, $P(s^{\alpha})$, $Q(s^{\alpha})$ and R are as follows*

$$z(t) = \Lambda E^{-1}x(t), \tag{45}$$

$$P(s^{\alpha}) = E\mathrm{diag}\left\{\Xi_1(s^{\alpha}), \Xi_2(s^{\alpha}), \dots, \Xi_m(s^{\alpha})\right\}, \tag{46}$$

$$Q(s^{\alpha}) = diag\left\{s^{r_1\alpha}, s^{r_2\alpha}, \ldots, s^{r_m\alpha}\right\} - \left[k_1^T, k_2^T, \ldots, k_m^T\right]^T E^{-1} P(s^{\alpha}), \tag{47}$$

$$R^T = ME^{-1}. \tag{48}$$

Define M_R as a matrix of $M_c = \left[B, AB, \ldots, A^{n-1}B\right]$ that consists of n-dimensional linearly independent columns,

$$M_R = \left[b_1, Ab_1, \ldots, A^{r_1-1}b_1, b_2, Ab_2, \ldots, A^{r_2-1}b_2, \ldots, b_m, Ab_m, \ldots, A^{r_m-1}b_m\right], \tag{49}$$

where $B = \left[b_1, b_2, \ldots, b_m\right]$, $r_i\,(i = 1, 2, \ldots, m)$ are the controllability indices of the system, and $r_1 + r_2 + \ldots + r_m = n$. Define

$$M_R^{-1} \triangleq \left[e_{11}^T, e_{12}^T, \ldots, e_{1r_1}^T, e_{21}^T, e_{22}^T, \ldots, e_{2r_2}^T, \ldots, e_{m1}^T, e_{m2}^T, \ldots, e_{mr_m}^T\right]^T, \tag{50}$$

where e_{ij} is an n-dimensional vector, the $n \times n$-order matrix E in (45-48) *can be obtained*

$$E^{-1} = \left[e_{1r_1}^T, A^T e_{1r_1}^T, \ldots, \left(A^{r_1-1}\right)^T e_{1r_1}^T, \ldots, e_{mr_m}^T, A^T e_{mr_m}^T, \ldots, \left(A^{r_m-1}\right)^T e_{mr_m}^T\right]^T. \tag{51}$$

Matrix Λ is an $m \times n$-order matrix and is expressed as

$$\Lambda = diag\left\{\Lambda_1, \Lambda_2, \ldots, \Lambda_m\right\}, \quad \Lambda_i = [1, 0, \ldots, 0] \in \mathbb{R}^{1\times r_i}, \tag{52}$$

Matrix M is an $m \times n$-order matrix, where the ($\sum_{j=1}^{i} r_j$)-th column is zero vector ($j = 1, 2, \ldots, m$), and the rank of the matrix comprised of other column vectors is $n - m$. $\Xi_i(s^{\alpha}) = \left[1, s^{\alpha}, \ldots, s^{(r_i-1)\alpha}\right]^T$ is m-dimensional column vectors, and k_i is the ($\sum_{j=1}^{i} r_j$)-th row in matrix $E^{-1}AE$.

Proof. Because system (23) is controllable, it must be able to be transformed into a controllable standard system[34] by using the full rank matrix E (defined as (51)). The transformed state $v(t) = E^{-1}x(t)$ satisfies

$$\mathscr{D}^{\alpha} v(t) = A_c v(t) + B_c u(t). \tag{53}$$

The state and input matrices have the following forms

$$A_c = diag\left\{A_{c1}, A_{c2}, \ldots, A_{cm}\right\} + K,$$
$$A_{ci} = \begin{bmatrix} 0 & 1 & \ldots & 0 \\ \vdots & \vdots & \ddots & \vdots \\ 0 & 0 & \ldots & 1 \\ 0 & 0 & \ldots & 0 \end{bmatrix}, \quad K = \Big[\underbrace{0, k_1^T}_{r_1}, \underbrace{0, k_2^T}_{r_2}, \ldots, \underbrace{0, k_m^T}_{r_m}\Big]^T, \ k_i \in \mathbb{R}^{1\times n}. \tag{54}$$

$$B_c = diag\left\{B_{c1}, B_{c2}, \ldots, B_{cm}\right\}, \quad B_{ci} = [0, \ldots, 0, 1]^T \in \mathbb{R}^{r_i\times 1}. \tag{55}$$

Reconsider (45) and take one item of it (such as $z_1(t)$) as an example. Evidently, $z_1(t) = [\Lambda_1, 0]\,E^{-1}x(t)$ and its Laplace transform is $Z_1(s) = [1, 0, \ldots, 0]\,E^{-1}X(s)$. Multiply this equation by s^{α} and substitute it into the original system (23) for simplification, until $s^{(r_1-1)\alpha}Z_1(s) = [0, \ldots, 1, \ldots, 0]\,E^{-1}X(s)$ is obtained, and there are a total of r_1 equations. Take Laplace transform of the other $z_i(t)$ and multiply it with the s^{α} factor until we obtain $s^{(r_i-1)\alpha}Z_i(s)$. All equations about $Z_i(s)$ in a matrix is expressed as

$$\begin{bmatrix} Z_1(s) \\ \vdots \\ s^{(r_1-1)\alpha}Z_1(s) \\ \vdots \\ Z_m(s) \\ \vdots \\ s^{(r_m-1)\alpha}Z_m(s) \end{bmatrix} = \begin{bmatrix} \Xi_1(s^{\alpha}) & & \\ & \ddots & \\ & & \Xi_m(s^{\alpha}) \end{bmatrix} Z(s) = \begin{bmatrix} I_{r_1} & & \\ & \ddots & \\ & & I_{r_m} \end{bmatrix} E^{-1}X(s). \tag{56}$$

Therefore, the specific form of the matrix $P(s^\alpha)$ can be obtained according to the definition.

Furthermore, we can obtain $r_i\alpha$th-order differential of $z_i(t)$ and obtain a Laplace transform of it, that is,

$$\begin{aligned} s^{r_i\alpha}Z(s) &= [0,\ldots,1,\ldots,0]\,A_cE^{-1}X(s) + [0,\ldots,1,\ldots,0]\,B_cU(s) \\ &= k_iE^{-1}X(s) + U_i(s) = k_iE^{-1}P(s^\alpha)Z(s) + U_i(s). \end{aligned} \tag{57}$$

Given that $U(s) = [U_1(s), U_2(s), \ldots, U_m(s)]$, the specific form of the matrix $Q(s^\alpha)$ can be written as defined by (47).

Finally, the way to find the matrix R is same as Theorem 1, without descriptions. ■

Remark 1. If the ith subsystem is defined as $\left(A_{ci} + \left[0, k_i^T\right]^T, B_{ci}\right)$, and the corresponding state variable is $v_i(t) = \left[v_{i1}(t), v_{i2}(t), \ldots, v_{ir_i}(t)\right]^T$, then the subsystem satisfies the state equation

$$\begin{cases} \mathscr{D}^\alpha v_{in}(t) = v_{i(n+1)}(t),\, n = 1,2,3,\ldots,r_i-1, \\ \mathscr{D}^\alpha v_{ir_i}(t) = k_i v(t) + u_i(t), \\ z_i(t) = v_{i1}(t). \end{cases} \tag{58}$$

Remark 2. The flat output of the selected system under these two theorems must be a linear combination of all system states according to Theorems 1 and 2.

In addition, there are other algorithms to find the flat output[27,28,35] of the FOS, and an example will be given below.

Definition 3. [35] The polynomial matrix $A(\lambda)$ is an $m \times n$-order matrix, where $m \le n$. $m \times m$-order full rank matrix $U(\lambda)$ and an $n \times n$-order full rank matrix $V(\lambda)$ are the Smith decomposition matrices of $A(\lambda)$ that satisfy

$$\bar{A}(\lambda) = U(\lambda)A(\lambda)V(\lambda) = [\Delta_m \;\; 0], \tag{59}$$

where Δ_m is an m-steps diagonal matrix, $\Delta_m = diag\{\delta_1, \delta_2, \ldots, \delta_r, 0, \ldots, 0\}$, $\delta_1|\delta_2\cdots|\delta_r$ is an invariable factor for $A(\lambda)$ and coefficient r is defined as $r = \text{rank}(A)$.

Lemma 4. *[28] The controllable commensurate fractional-order MIMO system* (23) *has a flat output $z(t)$ and its Laplace transform $Z(s)$ satisfies Lemma* 1*, among them*

$$R^T = \left[\, O_m \;\; 1 \,\right] U_B, \tag{60}$$

$$P(s^\alpha) = V_F(s^\alpha)\begin{bmatrix} O_m \\ 1 \end{bmatrix}, \tag{61}$$

$$Q(s^\alpha) = B_L^{-1}\left[s^\alpha I_n - A\right]P(s^\alpha), \tag{62}$$

where U_B is a Smith decomposition matrix for B, and V_F is a decomposition matrix of $R^T[s^\alpha I_n - A]$. B_L^{-1} is the left inverse matrix of B, that is,

$$\overline{B} \triangleq U_B B V_B = \begin{bmatrix} I_m \\ 0 \end{bmatrix}, \tag{63}$$

$$\overline{F}(s^\alpha) \triangleq U_F(s^\alpha)R^T\left[s^\alpha I_n - A\right]V_F(s^\alpha) = \left[\, \Delta_m \;\; 0 \,\right], \tag{64}$$

$$B_L^{-1}B = I_m. \tag{65}$$

The lemma is a constructive lemma. By comparing with Theorems 1 and 2, this conclusion is more complex, because two Smith decomposition matrices required for solving, and matrix $P(s^\alpha)$ may contain αth-order differential terms. Therefore, it is not as convenient as the former in the design of the ADRC controller.

3.3 | Differential flatness-based ADRC scheme for underactuated FOSs

Consider the following controllable underactuated commensurate FOS with $0 < \alpha < 1$

$$\begin{cases} \mathscr{D}^{\alpha} x(t) = Ax(t) + Bu(t), \\ y(t) = Cx(t), \end{cases} \tag{66}$$

where $A \in \mathbb{R}^{n \times n}$, $B \in \mathbb{R}^{n \times m}$, $C \in \mathbb{R}^{r \times n}$, $n \geq m$, and $r > m$.

Obtain the corresponding E, Λ, A_c, B_c, $P(s^{\alpha})$, $Q(s^{\alpha})$ and matrix R according to Theorem 2 and Remark 1, then the flat output of system (66) is $z(t) = \Lambda E^{-1} x(t) = [z_1(t), z_2(t), \dots, z_m(t)]^T$. In the ith subsystem, assume $z_i(t) = v_{i1}(t)$, that is,

$$z_i(t) = v_{i1}(t),\ \mathscr{D}^{\alpha} z_i(t) = v_{i2}(t),\ \dots,\ \mathscr{D}^{\alpha r_i} z_i(t) = f_i(v(t)) + u_i(t). \tag{67}$$

Let $h_i(t) = z_i(t)$ be the output of this subsystem, if the subsystem contains the disturbance $w_i(t)$, the state space equation can be written as

$$\begin{cases} \mathscr{D}^{\alpha} v_{in}(t) = v_{i(n+1)}(t), n = 1, 2, 3, \dots, r_i - 1, \\ \mathscr{D}^{\alpha} v_{ir_i}(t) = f_i(v(t)) + u_i(t) + w_i(t), \\ h_i(t) = v_{i1}(t). \end{cases} \tag{68}$$

$f_i(v(t)) = k_i v(t)$ is used as a known or unknown function in this subsystem, then an FOESO is designed for system (68)

$$\begin{cases} \mathscr{D}^{\alpha} \hat{z}_{in}(t) = \hat{z}_{i(n+1)}(t) - \beta_{in} e_{in}(t), n = 1, 2, 3, \dots, r_i - 1, \\ \mathscr{D}^{\alpha} \hat{z}_{ir_i}(t) = \hat{z}_{i(n+1)}(t) - \beta_{ir_i} e_{ir_i}(t) + u_i(t), \\ \mathscr{D}^{\alpha} \hat{z}_{i(r_i+1)}(t) = -\beta_{i(r_i+1)} e_{i(r_i+1)}(t), \end{cases} \tag{69}$$

where $\hat{z}_{ij}(t), j = 1, 2, \cdots, r_i, r_i + 1$ is the extended observation state of system (68), $e_{ij}(t) = \hat{z}_{ij}(t) - v_{ij}(t)$ are error, according to section 2.3, select

$$\beta_{ij} = C^{j}_{r_i+1} \omega^{j}_{i0}, \quad i = 1, 2, \dots, m, \quad j = 1, 2, \dots, r_i. \tag{70}$$

Then, the $PI^{\lambda}D^{\alpha}$ controller (16-17) is designed for the ith subsystem

$$u_i(t) = u_{i0}(t) - \hat{z}_{i(r_i+1)}(t),\ \mathscr{D}^{\alpha r_i} h_i(t) \approx u_{i0}(t). \tag{71}$$

$u_{i0}(t)$ is designed as a $PI^{\lambda}D^{\alpha}$ controller, and the differential signal is generated by the FOTD. The output signal $h_i(t)$ of the ith subsystem can be approximated by (71). For the subsystems of $i = 1, 2, \dots, m$, the above FOESO and control scheme are introduced. Finally, the total output signal is $h(t) = \left[h_1(t), h_2(t), \dots, h_m(t)\right]^T$. Given that $h_i(t) = z_i(t)$, the flat output of system (66) $z(t) = h(t)$ can be obtained by the above steps. Substitute (45) into the output equation of system (66), that is,

$$Y(s) = CX(s) = CP(s^{\alpha}) H(s). \tag{72}$$

Inverse transform to the input reference signal $r(t)$, then the reference input signal $v(t)$ for flat output signals can be obtained, among them, inverse transformation matrix $\left(CE\Lambda^T\right)^{-1}_{\mathrm{R}}$ is the right inverse matrix of $CE\Lambda^T$.

The block diagram of the controlled system is shown in Figure 3.

It should be noted that in many instances, system state variables $x_i(t), i = 1, 2, \dots, n$ are not all actually measured. Because the flat output designed according to Theorems 1 and 2 is linear combination of all state variables, but the flat output $z(t)$ may contain variables $x_i(t)$ that cannot be measured. It causes difficulties in selecting and using flat output in the actual project. In actual design and implementation, there are two ways to solve the above problems.

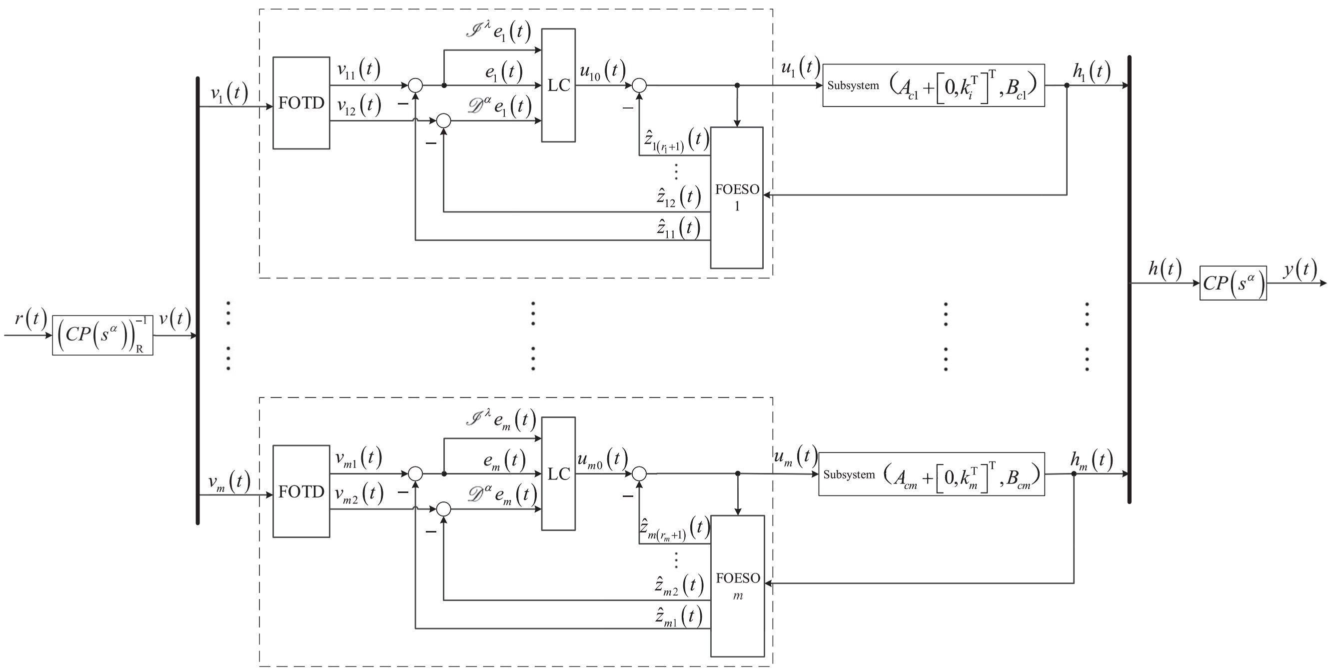

FIGURE 3 Differential flatness-based ADRC scheme for underactuated fractional-order systems

The first method is to introduce a full-dimensional or reduced-dimensional state observer, then we estimate the state variables that cannot be obtained by measurement and substitute the estimated values into the flat output expression. Taking the flat output of a multiinput system as an example, (45) should be rewritten as $z(t) = \Lambda E^{-1}\left[x_O(t) + \hat{x}_{\bar{O}}(t)\right]$, where $x_O(t)$ is the part of the system state that can be directly measured in the original system (23) or obtained by exporting $y(t)$, $\hat{x}_{\bar{O}}(t)$ is the estimated value of the remaining nondirectly available system state $x_{\bar{O}}(t)$. The total states of the system can be expressed as $x(t) = x_O(t) + x_{\bar{O}}(t)$.

On the other hand, output equations are not used when designing the flat output. A new output equation $y_O(t) = C_O x(t) = I_n x(t) = x(t)$ can be added and is composed of a new system with the state equation (23). The output of the system is composed of all the states of the original system. The corresponding flat output $z(t)$ can be obtained by substituting this state into the flat output expression (30) or (45).

4 | SIMULATION EXAMPLE

The existing literature[36] gives a fractional-order model of an elevated crane, and the model is shown in Figure 4.

$$\begin{cases} \mathscr{D}^{\alpha}x(t) = \begin{bmatrix} 0 & 1 & 0 & 0 \\ 0 & 0 & 0 & mg/M \\ 0 & 0 & 0 & 1 \\ 0 & 0 & -(M+m)g/Ml & 0 \end{bmatrix} x(t) + \begin{bmatrix} 0 \\ 1/M \\ 0 \\ -1/Ml \end{bmatrix} u(t), \\ y(t) = \begin{bmatrix} 1 & 0 & 0 & 0 \\ 0 & 0 & 1 & 0 \end{bmatrix} x(t), \end{cases}$$

where $x(t) = \left[d(t), \mathscr{D}^{\alpha}d(t), \theta(t), \mathscr{D}^{\alpha}\theta(t)\right] \triangleq [x_1(t), x_2(t), x_3(t), x_4(t)]$ is the distance between the crane and the wall $d(t)$, αth-order differential of distance, the angle between the load and the crane $\theta(t)$, and αth-order differential of included angle.

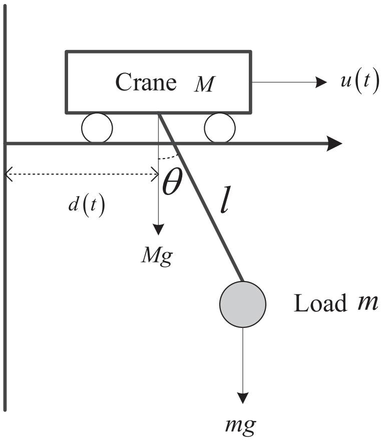

FIGURE 4 Schematic diagram of an overhead crane

The input signal $u(t)$ is the lateral force loaded on the crane; M and m is the quality of the crane and the quality of the load, respectively; l is the length of the connecting line between the load and the crane; g is gravity acceleration; and the system order α satisfies $0 < \alpha < 1$.

This system is a commensurate underactuated FOS, and the dimensions of the system are $n = 4, m = 1$, and $r = 2$. The parameters of the system is assumed as $M = 0.5kg$, $m = 4kg$, $l = 2.4m$, $\alpha = 0.4$, and the value of g is $9.8m/s^2$. It can be found that this system is a fully controllable FOS via calculations. According to Theorem 1, the flat output is

$$\begin{aligned} z(t) &= [1, 0, 0, 0]\, T^{-1} M_c^{-1} x(t) \\ &= 0.0136x_1(t) + 0.0121x_2(t) - 0.9155x_3(t) + 0.0290x_4(t). \end{aligned} \tag{73}$$

Matrices $P(s^\alpha)$, R, and $Q(s^\alpha)$ are

$$P(s^\alpha) = \begin{bmatrix} 73.50 - 66.33s^\alpha + 2s^{2\alpha} \\ 73.50s^\alpha - 66.33s^{2\alpha} + 2s^{3\alpha} \\ -0.83s^{2\alpha} \\ -0.83s^{3\alpha} \end{bmatrix}, \quad R = \begin{bmatrix} 0.0136 \\ 0.0257 \\ -3.1822 \\ 0.0617 \end{bmatrix},$$
$$Q(s^\alpha) = 36.75 + s^{4\alpha}. \tag{74}$$

The flat output $z(t)$ is a linear combination of states $d(t)$, $\mathscr{D}^\alpha d(t)$, $\theta(t)$, and $\mathscr{D}^\alpha \theta(t)$ by observation. In actual engineering, parameters $x_1(t) = d(t)$ and $x_3(t) = \theta(t)$ are two output variables that can be directly measured, and the two remaining state variables cannot be measured directly, but the output matrix can be expanded. Let the output matrix be $C_O = I_4$ to obtain all state variables in system (73) and these state variables are substituted into the flat output calculation.

If the system needs to track a square wave signal. The amplitude of the square wave signal is 2, and the angle reference signal is always zero, then the tracking signals of its displacement and angle and the αth-order differential tracking signals of the displacement and angle can be generated by an FOTD. To ensure tracking speed and system kickback, the amplitude of the input control signal is $r = 1$, and the gain of the hyperbolic tangent function is $k = 1$. It is easy to construct a reference tracking signal relative to the flat output $z(t)$ by using the tracking signal generated by FOTD, and this signal will also be used in the design of the FOESO and the selection of control schemes.

Consider a system with flat output as an output variable. A new set of variables $v_1(t) = z(t)$, $v_2(t) = \mathscr{D}^\alpha z(t)$, $v_3(t) = \mathscr{D}^{2\alpha} z(t)$, and $v_4(t) = \mathscr{D}^{3\alpha} z(t)$ is defined, then use these four new variables as state variables, $h(t) = z(t)$ is the output, and system (73) can be rewritten as

$$\begin{cases} \mathscr{D}^\alpha v_1(t) = v_2(t), \\ \mathscr{D}^\alpha v_2(t) = v_3(t), \\ \mathscr{D}^\alpha v_3(t) = v_4(t), \\ \mathscr{D}^\alpha v_4(t) = f(v(t)) + u(t) + w(t), \\ h(t) = v_1(t), \end{cases} \tag{75}$$

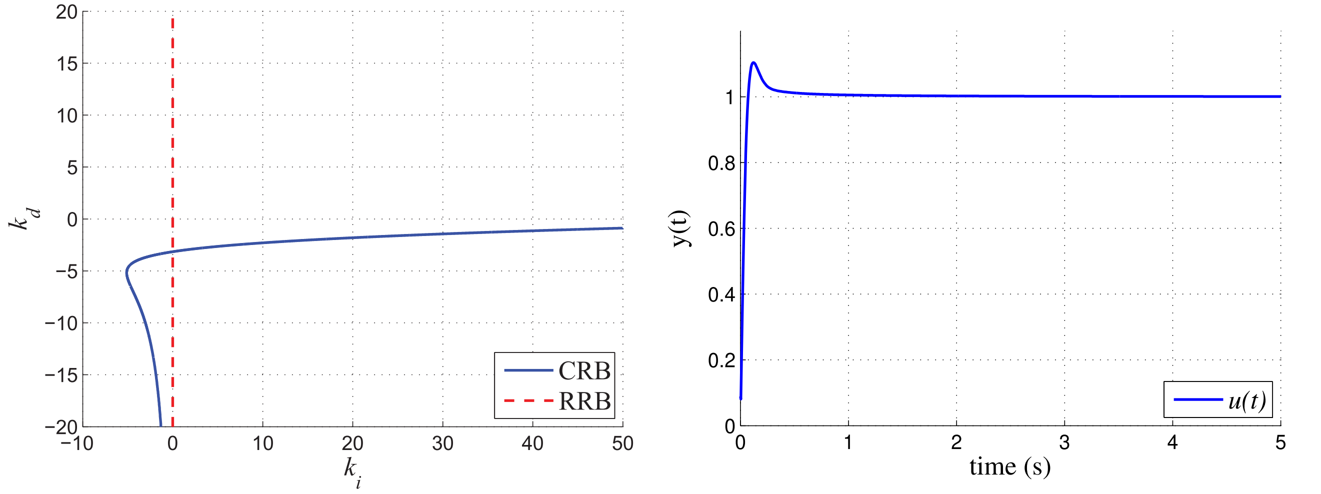

FIGURE 5 Controller parameters complex root boundary-real root boundary curve and ideal closed-loop step response of the system under $\lambda = 0.5$, $k_p = 10$, $k_i = 10$, $k_d = 50$ conditions [Colour figure can be viewed at wileyonlinelibrary.com]

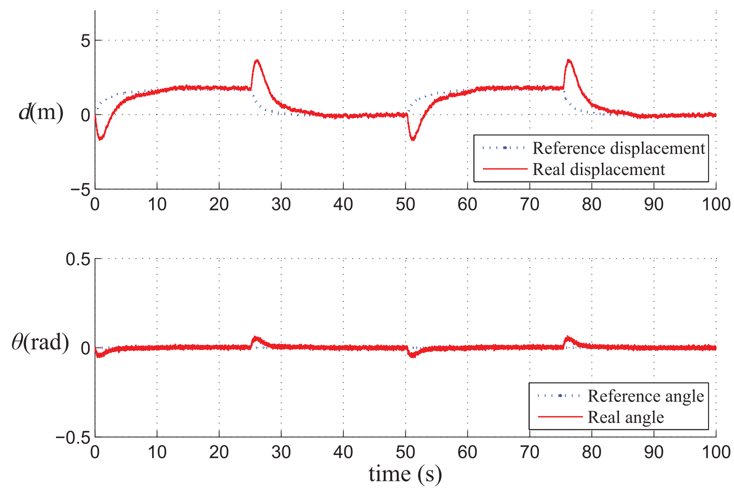

FIGURE 6 System reference input signal and output signal [Colour figure can be viewed at wileyonlinelibrary.com]

$f(v(t)) = -36.75v_3(t)$ can be obtained by calculating, and $w(t)$ is the unknown external disturbance of the system. An FOESO is constructed for system (75)

$$\begin{cases} \mathscr{D}^{\alpha}\hat{z}_1(t) = \hat{z}_2(t) - \beta_1 e_1(t), \\ \mathscr{D}^{\alpha}\hat{z}_2(t) = \hat{z}_3(t) - \beta_2 e_1(t), \\ \mathscr{D}^{\alpha}\hat{z}_3(t) = \hat{z}_4(t) - \beta_3 e_1(t), \\ \mathscr{D}^{\alpha}\hat{z}_4(t) = \hat{z}_5(t) - \beta_4 e_1(t) + u(t), \\ \mathscr{D}^{\alpha}\hat{z}_5(t) = -\beta_5 e_1(t), \end{cases} \tag{76}$$

where $\beta_1 = 5\omega_0$, $\beta_2 = 10\omega_0^2$, $\beta_3 = 10\omega_0^3$, $\beta_4 = 5\omega_0^4$, and $\beta_5 = \omega_0^5$.

Controller $u_0(t)$ is selected as the $PI^{\lambda}D^{\mu}$ controller. It can be determined that there are stable controller parameters when the system order $0 < \alpha < 2/3$ according to Corollary 1, evidently $\alpha = 0.4$ in this example satisfies the conditions in Corollary 1. The RRB curve and imaginary root boundary curve of the controller parameters for $\lambda = 0.5$ and $k_p = 10$ is shown Figure 5, and the area enclosed by the red line and the blue line in the first quadrant of the (k_i, k_d) plane is the stably domain of the controller parameters. Substituting $k_i = 10$ and $k_d = 50$ into (19) to obtain the step response of an ideal closed-loop system, as shown in Figure 5.

The reference displacement input signal is selected as a square wave, the amplitude is 2, the period is 16π, and the reference angle signal is always zero. If white noise is observed when measuring the position signal and the

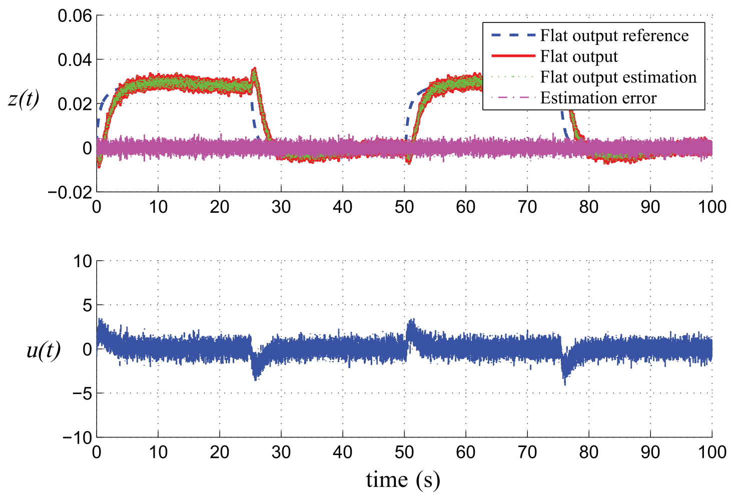

FIGURE 7 System flat output signal and control signal [Colour figure can be viewed at wileyonlinelibrary.com]

angle signal of the system, then the final output displacement and angle of the system are shown in Figure 6. Among them, the reference displacement signal is the tracking signal of the square wave signal after passing through the designed FOTD. The system will have a short period of jitter when the desired displacement changes, but the reference signal can be quickly tracked within 5seconds and almost constantly, the system has a small angular offset, and the angle remains almost unchanged at 0 *rad*.

In addition, the flat output of the system reference input signal, the flat output signal of the actual system, the flat output observed by the FOESO, the error signal between the actual flat output and the flat output observed by the observer, and the input control signal are shown in Figure 7. The flat output cannot only rapidly track the reference signal, but also has a small overshoot. At the same time, the observation error of the FOESO on the flat output signal is also very small, and the system performs well.

5 | CONCLUSIONS

In this article, FOTD and FOESO are used to construct the control framework for the FOADRC based on the $PI^{\lambda}D^{\mu}$ control. The necessary conditions for the controller to ensure system stability is given. The FOADRC scheme based on differential flatness for underactuated FOSs is proposed. A set of flat output expressions with a fixed format can be given under the controllable conditions of the system, and making the flat output as the equivalent of the system output simply and easy to analyze and calculate. Then the FOADRC scheme of the system is designed by using the flat output. Finally, the concrete implementation steps and simulation results of the FOADRC scheme are given through the simulation example, and the effectiveness of the proposed scheme in this article is verified.

ORCID

Yong Wang https://orcid.org/0000-0002-6773-6544

REFERENCES

1. Sun HG, Zhang Y, Baleanu D, Chen W, Chen Y. A new collection of real world applications of fractional calculus in science and engineering. *Commun Nonlinear Sci Numer Simul*. 2018;64:213-231.
2. Cui RZ, Wei YH, Chen YQ, Cheng SS, Wang Y. An innovative parameter estimation for fractional-order systems in the presence of outliers. *Nonlinear Dyn*. 2017;89(1):453-463.
3. Wei YH, Wang JC, Liu TY, Wang Y. Sufficient and necessary conditions for stabilizing singular fractional order systems with partially measurable state. *J Franklin Inst*. 2019;356(4):1975-1990.
4. Taghavian H, Tavazoei MS. Robust stability analysis of uncertain multiorder fractional systems: young and Jensen inequalities approach. *Int J Robust Nonlinear Control*. 2018;28(4):1127-1144.
5. Alaviyan Shahri ES, Alfi A, Tenreiro Machado JA. Stability analysis of a class of nonlinear fractional-order systems under control input saturation. *Int J Robust Nonlinear Control*. 2018;28(7):2887-2905.
6. Chen Y, Wei Y, Zhong H, Wang Y. Sliding mode control with a second-order switching law for a class of nonlinear fractional order systems. *Nonlinear Dyn*. 2016;85(1):633-643.

7. Chen Y, Wei Y, Zhou X, Wang Y. Stability for nonlinear fractional order systems: an indirect approach. *Nonlinear Dyn*. 2017;89(2):1011-1018.
8. Zheng S, Tang X, Song B. Graphical tuning method of FOPID controllers for fractional order uncertain system achieving robust-stability. *Int J Robust Nonlinear Control*. 2016;26(5):1112-1142.
9. Wei Y, Sheng D, Chen Y, Wang Y. Fractional order chattering-free robust adaptive backstepping control technique. *Nonlinear Dyn*. 2019;95(3):2383-2394.
10. Ahmed S, Wang H, Tian Y. Robust adaptive fractional-order terminal sliding mode control for lower-limb exoskeleton. *Asian J Control*. 2019;21(1):473-482.
11. Machado JAT, Moghaddam BP. A robust algorithm for nonlinear variable-order fractional control systems with delay. *Int J Nonlinear Sci Numer Simul*. 2018;19(3-4):1-8.
12. Feytout B, Lanusse P, Sabatier J, Gracia S. Robust CRONE design for a variable ratio planetary gearing in a variable speed wind turbine. *Asian J Control*. 2013;15(3):806-818.
13. Han JQ. Active disturbance rejection controller and its application. *Control Decis*. 1998;13(1):19-23.
14. Huang Y, Zhang WG. Development of active disturbance rejection controller. *Control Theory Appl*. 2002;19(4):485-492.
15. Gao Z. Active disturbance rejection control: a paradigm shift in feedback control system design. Paper presented at: Proceedings of the 2006, American Control Conference (ACC 2006); June 14–16, 2006:2399-2405; Minneapolis, MN.
16. Li M, Li DH, Wang J, Zhao CZ. Active disturbance rejection control for fractional-order system. *ISA Trans*. 2013;52(3):365-374.
17. Erenturk K. Fractional-order $PI^{\lambda}D^{\mu}$ and active disturbance rejection control of nonlinear two-mass drive system. *IEEE Trans Ind Electron*. 2013;60(9):3806-3813.
18. Yang J, Dong L, Liao X. Fractional order PD controller based on ADRC algorithm for DC motor. Paper presented at: Proceedings of the 2014, IEEE Conference and Expo Transportation Electrification Asia-Pacific (ITEC Asia-Pacific 2014); 2014:1-6; Beijing, China.
19. Sun JF, Shan L, Qi ZD, Qu YX, Li J. Fractional order ADRC algorithm to ship servo system. Paper presented at: Proceedings of the 2016 35th Chinese Control Conference (CCC 2016); 2016:1086-1091; Chengdu, China.
20. Wei YH, Du B, Cheng SS, Wang Y. Fractional order systems time-optimal control and its application. *J Optim Theory Appl*. 2017;174(1):122-138.
21. Wei YH, Gao Q, Chen YQ, Wang Y. Design and implementation of fractional differentiators, part I: system based methods. *Control Eng Pract*. 2019;84:297-304.
22. Gao Z. Active disturbance rejection control for nonlinear fractional-order systems. *Int J Robust Nonlinear Control*. 2016;26(4):876-892.
23. Gao Z, Liao X. Active disturbance rejection control for synchronization of different fractional-order chaotic systems. Paper presented at: Proceeding of the 11th World Congress on Intelligent Control and Automation (WCICA 2014); 2014:2699-2704; Shenyang, China.
24. Pan J, Qi S, Wang Y. Flatness based active disturbance rejection control for cart inverted pendulum and experimental study. Paper presented at: Proceedings of the 2015 American Control Conference (ACC 2015); 2015:4868-4873; Chicago, IL.
25. Victor S, Melchior P, Oustaloup A. Robust path tracking using flatness for fractional linear MIMO systems: a thermal application. *Comput Math Appl*. 2010;59(5):1667-1678. Fractional Differentiation and Its Applications.
26. Victor S, Melchior P, Oustaloup A. Computation of flat outputs for fractional systems: a thermal application. *IFAC Proc Vol*. 2013;46(1):42-47.
27. Victor S, Melchior P, Lévine J, Oustaloup A. Flatness for linear fractional systems with application to a thermal system. *Automatica*. 2015;57:213-221.
28. Victor S, Melchior P, Malti R, Oustaloup A. Path tracking with flatness and CRONE control for fractional systems: thermal application. *IFAC Proc Vol*. 2011;44(1):10818-10823.
29. Sira-Ramirez H, Agrawal SK. *Differentially Flat Systems*. Boca Raton, FL: CRC Press; 2004.
30. Podlubny I. Fractional-order systems and $PI^{\lambda}D^{\mu}$ controllers. *IEEE Trans Autom Control*. 1999;44(1):208-214.
31. Wei Y, Dai Y, Cheng S, Jia T, Wang Y. Study on fractional order tracking differentiator. Paper presented at: Proceedings of the 5th Conference on Nonlinear Science and Complexity (NSC 2014); 2014:04; Xian, China.
32. Ackermann J, Kaesbauer D. Stable polyhedra in parameter space. *Automatica*. 2003;39(5):937-943.
33. Monje CA, Chen YQ, Vinagre BM, Xue DY, Feliu-Batlle V. *Fractional Order Systems and Controls: Fundamentals and Applications*. London, UK: Springer; 2010.
34. Koussiouris TG. Controllability indices of a system, minimal indices of its transfer function matrix and their relations. *Int J Control*. 1981;34(3):613-622.
35. Smith HJS. On systems of linear indeterminate equations and congruences. *Philos Trans R Soc Lond*. 1861;151:293-326.
36. Srivastava T, Singh AP, Agarwal H. Modeling the under-actuated mechanical system with fractional order derivative. *Progr Fract Differ Appl*. 2015;1(1):57-64.

How to cite this article: Li Z, Wei Y, Zhou X, Wang J, Wang J, Wang Y. Differential flatness-based ADRC scheme for underactuated fractional-order systems. *Int J Robust Nonlinear Control*. 2020;30:2832–2849. https://doi.org/10.1002/rnc.4905